Macromolecular Rapid Communications
www.mrc-journal.de

A Systematic Study on Biobased Epoxy-Alcohol Networks: Highlighting the Advantage of Step-Growth Polyaddition over Chain-Growth Cationic Photopolymerization

*Antonella Fantoni, Thomas Koch, Robert Liska, and Stefan Baudis**

Vanillyl alcohol has emerged as a widely used building block for the development of biobased monomers. More specifically, the cationic (photo-)polymerization of the respective diglycidyl ether (DGEVA) is known to produce materials of outstanding thermomechanical performance. Generally, chain transfer agents (CTAs) are of interest in cationic resins not only because they lead to more homogeneous polymer networks but also because they strikingly improve the polymerization speed. Herein, the aim is to compare the cationic chain-growth photopolymerization with the thermally initiated anionic step-growth polymerization, with and without the addition of CTAs. Indeed, CTAs lead to faster polymerization reactions as well as the formation of more homogeneous networks, especially in the case of the thermal anionic step-growth polymerization. Resulting from curing above the T_G of the respective anionic step-growth polymer, materials with outstanding tensile toughness (>5 MJ cm^{-3}) are obtained that result in the manufacture of potential shape-memory polymers.

1. Introduction

In recent years, an increasing demand to replace petroleum derived polymers has been witnessed. Both the predicted scarcity of petroleum resources as well as growing environmental concerns are driving forces for the development of novel and sustainable material platforms.[1–3] Consequentially, the design of biobased polymers is receiving evermore attention as environmentally friendly alternatives are becoming essentially more attractive to the petroleum-based counterparts. Today, thermosetting polymers make up to 20% of the worldwide plastic production.[3] Herein, epoxy resins represent the most important class of monomers, making up roughly 70% of all thermosets[3,4] as a result of their outstanding mechanical properties, good thermal stability and processability.[5] The majority of such materials is obtained from the reaction of bisphenol A (BPA) and epichlorohydrin, giving the diglycidyl ether of BPA (BADGE). Although there is no renewable source for BPA, Dow Glycerin to Epichlorohydrin Technologies and Solvay Epicerol have reported the production of epichlorohydrin from glycerol, a by-product in the biodiesel industry.[6] Furthermore, BPA is known to act as an estrogen mimic and was recently declared as a carcinogenic mutagen and reprotoxic,[7] promoting the search for both nontoxic and renewable alternatives.

Over the last decade, a plethora of renewable building blocks has been examined and reported in literature. Among those, epoxidized vegetable oils have already been commercialized and are thus frequently used. Unfortunately, low cross-linking densities and flexibility stemming from the long hydrocarbon chains result in unsatisfactory thermomechanical properties (e.g., low T_G).[8–10] By the use of more rigid cycloaliphatic and aromatic structures, this problem can be resolved. Hence, Mantzaridis et al. prepared bioderived modified rosin acid oligomers into BPA-free epoxy resins with high T_G of >90 °C when crosslinked with diamines.[11] Another widely used building block from renewable resources is the saccharide-derived isosorbide.[12–14] Crosslinking of the diglycidyl ether with isophorone diamine gave materials with enhanced thermomechanical properties. However, the hygroscopic nature of the monomer might have a negative impact on polymer properties.

Although the aforementioned examples proved that renewable building blocks can be used to fabricate sustainable epoxy resins, they did not reach the thermomechanical properties attained by the aromatic BADGE. Hence, the design of aromatic bio-based building blocks receives evermore attention among the scientific community. Herein, lignin represents the most abundant aromatic feedstock in nature.[15] By the chemical

A. Fantoni, S. Baudis
Christian Doppler Laboratory for Advanced Polymers for Biomaterials and 3D Printing
Getreidemarkt 9, Vienna 1060, Austria
E-mail: stefan.baudis@tuwien.ac.at
A. Fantoni, R. Liska, S. Baudis
Institute of Applied Synthetic Chemistry
Technische Universität Wien
Vienna 1060, Austria
T. Koch
Institute of Materials Science and Technology
Technische Universität Wien
Vienna 1060, Austria

The ORCID identification number(s) for the author(s) of this article can be found under https://doi.org/10.1002/marc.202400323

DOI: 10.1002/marc.202400323

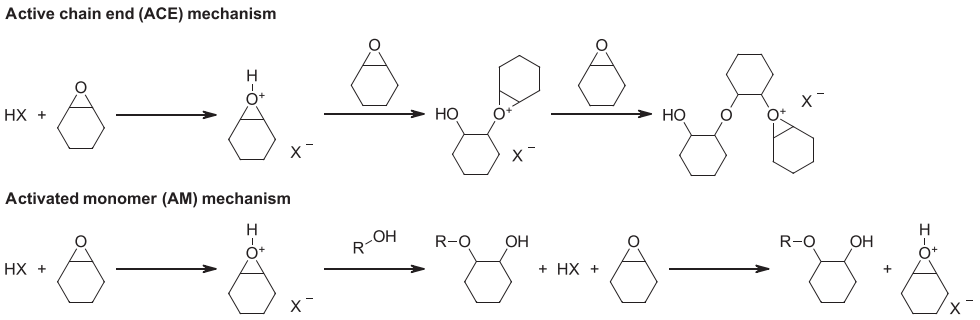

Figure 1. Schematic overview of possible propagation mechanisms in cationic polymerization: ACE (top) and AM (bottom) of epoxides. Cyclohexene oxide is used as model monomer.

depolymerization of the highly crosslinked polyphenolic lignin structure, a variety of phenol-based precursor molecules, e.g. vanillin, can be obtained. More specifically, roughly 15% of today's vanillin production is based on the lignin-to-vanillin process, making vanillin an ideal bio-derived precursor for epoxy resins.[16] Over the last decade, the group of Caillol demonstrated that vanillin can be converted into multiple mono- and multifunctional epoxy monomers.[16,17] Furthermore, Wang et al. prepared lignin-reinforced vanillyl alcohol-based nanocomposite materials that were crosslinked with triethylenetetramine.[18] The composites displayed high tensile strength (up to 60 MPa) and improved tensile toughness compared to the neat epoxy-amine polyadduct. Furthermore, Savonnet et al. prepared di-, tri- and tetrafunctional glycidyl ethers of vanillin by an oxidative coupling reaction.[19] Polymerization of the multifunctional synthons with a cycloaliphatic diamine resulted in high T_G materials (140–200 °C). Finally, a recent publication by Dinu et al. demonstrated the possible application of vanillin-derived epoxy resins for aerospace and space sectors.[20] Copolymerization of the diglycidyl ether of vanillyl alcohol (DGEVA) with anhydrides catalyzed by imidazoles gave high performance materials (T_G > 100 °C, $G'_{30\,°C} \approx 3$ GPa). While the main focus lies on the thermal curing of vanillin-derived epoxy resins, Sangermano et al. reported the synthesis and cationic photopolymerization of DGEVA.[21] High curing speed and reduced energy consumption of the UV-curing process additionally decrease the environmental aspect of bio-derived resins, thus making cationic photopolymerization of epoxy monomers even more eco-friendly.

Unfortunately, both thermal and photopolymerization of epoxy monomers still suffer from several disadvantages. Thermally curable formulations exhibit poor storage stability and demand high processing temperatures. By contrast, radiation curing can be performed at ambient temperatures. Nevertheless, highly crosslinked and thus irregular polymer networks are obtained.[22]

Regarding the cationic photopolymerization, two different mechanisms are observed and well-described in literature for the (photo-)acid-catalyzed epoxy polymerization. On the one hand, the polymerization proceeds via the conventional active chain-end (ACE) mechanism, where new monomers react immediately with the cationic (active) end of the growing polymer chain (**Figure 1**, top). Additionally, the activated monomer (AM) mechanism was proposed by Kubisa and Penczek.[23,24] Here, the active center is transferred away from the growing chain and the AM is attacked by nucleophilic substances such as water or alcohols (Figure 1, bottom).

It was previously shown by Dillan and Jessop, that the addition of hydroxyl species enhances the rate of polymerization but decreases the final T_G of the chain-growth polymers.[25] Interestingly, difunctional CTAs decreased the T_G of the polymers less than mono-ols. Additionally, a comparison between different substituents on the hydroxyl components showed that primary alcohols proved to be the most potent chain transfer agents (CTAs) as a result of the least steric hindrance.

By contrast, very few reports have been published on thermally curable epoxy-alcohol polyadducts. Kropka and co-workers investigated the reaction kinetics of epoxy monomers with hydroxyl donors.[26] It was assumed that the reaction mechanism is shifted towards a step-growth polymerization, giving more homogeneous networks. In recent studies from our group, the base-catalyzed reaction between alcohols and epoxides was studied in detail (**Figure 2**).[27,28] It was shown, that imidazoles enable an alternating co-polymerization between both moieties, where the monomer reacts exclusively with one another to give —AB— polyadducts. Investigations on the thermomechanical properties indicated that by the use of epoxy-alcohol polyaddition polymers with sharp glass transitions and high tensile toughness could be obtained.

Herein we aim to further investigate both the light induced cationic photopolymerization (chain-growth, **Figure 3b**) as well as the base catalyzed thermal polyaddition (step-growth, Figure 3c) of vanillyl alcohol-derived epoxy monomers with equimolar amounts of aliphatic hydroxyl comonomers. At first, a kinetic proton NMR study was conducted to gather insights about the conversion of both monomers in photochemical and thermally induced polyreactions. Therefore, a monofunctional epoxide (phenyl glycidyl ether, PGE) was reacted with *n*-hexanol to give linear photopolymers via a light induced chain-growth AM mechanism. By contrast, thermally induced step-growth polyaddition of DGEVA was studied with hexanediol. Thereafter, (photo-)DSC measurements combined with FT-IR were used to investigate the reactivity and curing behavior of crosslinked DGEVA resins. Additionally, an extensive comparison between the acid/base-catalyzed alcohol-epoxy and neat acid/base-initiated epoxy polymers was performed. Finally, dynamic mechanical thermoanalysis and tensile tests were employed to assess the thermomechanical properties of bio-based polymers.

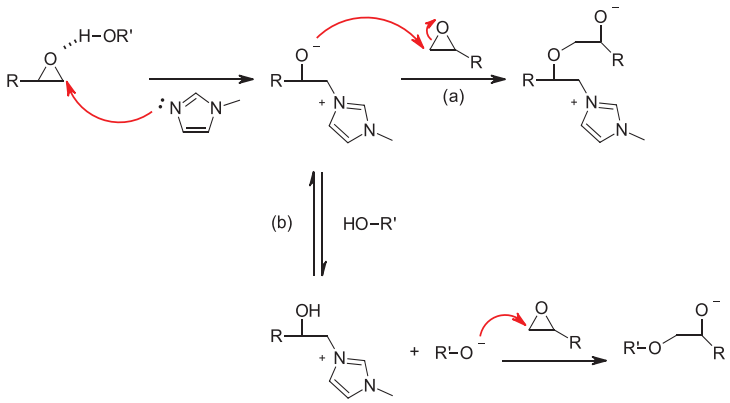

Figure 2. a) Expected mechanism of initiation of the anionic ring-opening polymerization of epoxides and b) chain-transfer in the presence of hydroxyl groups to facilitate epoxy-alcohol polyaddition.[29]

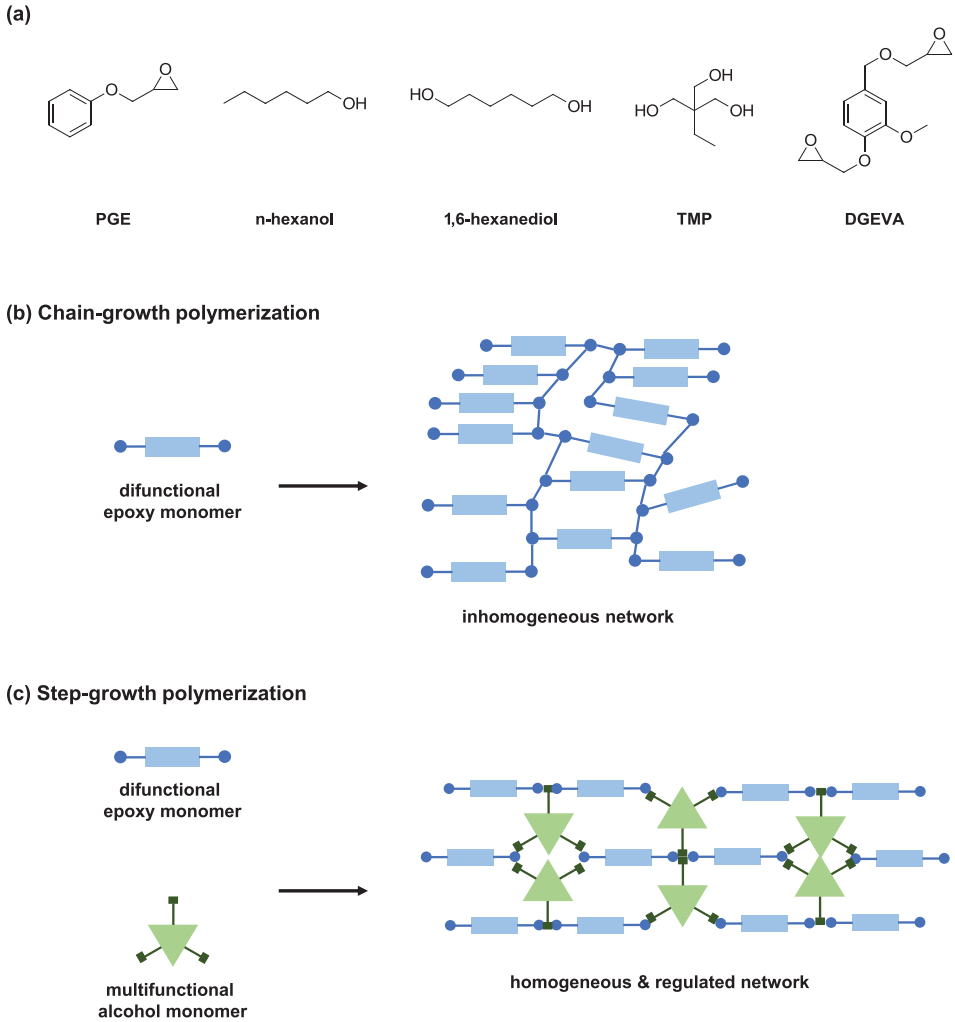

Figure 3. a) Monomers used in this study: phenyl glycidyl ether (PGE), n-hexanol, 1,6-hexanediol, trimethylolpropane (TMP) and diglycidyl ether of vanillyl alcohol (DGEVA). Schematic representation of the network architecture of b) the chain-growth polymerization of difunctional epoxy monomers and c) the step-growth polymerization of epoxy monomers with multifunctional alcohols.

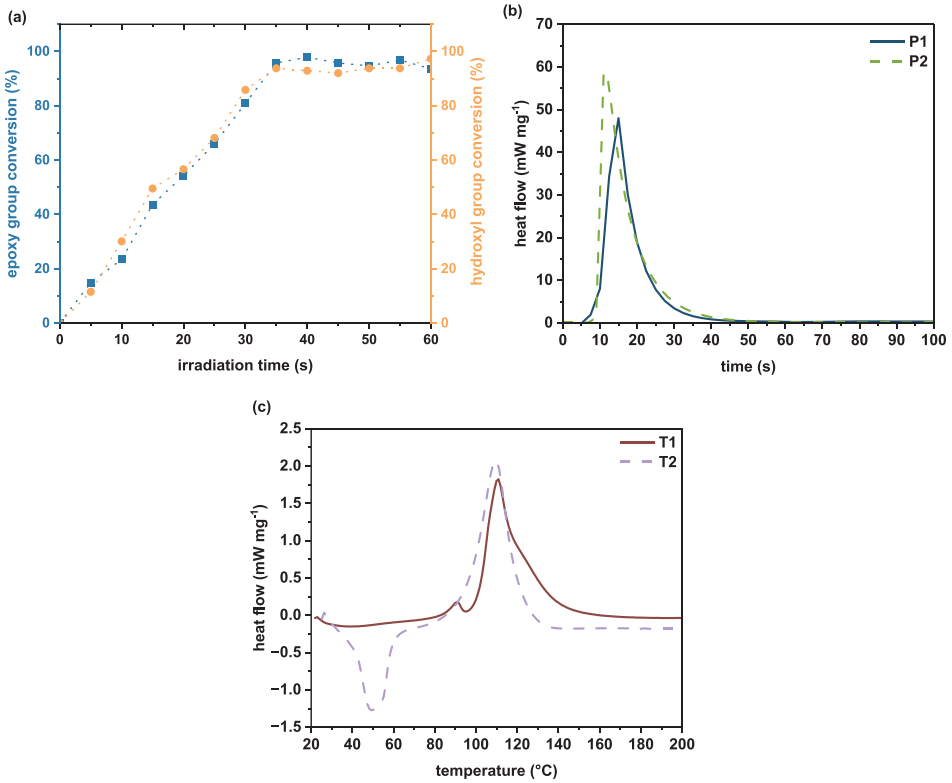

Figure 4. a) Conversion of epoxy groups (blue squares) of PGE and hydroxyl groups of n-hexanol (orange circles) from ^{1}H-NMR measurements of photo-DSC samples using 1 wt% of UVI6976 as initiator. For better visibility, the symbols were connected with dotted lines. b) Photo-DSC measurements of DGEVA without (P**1**, blue solid) and with (P**2**, green dashed) TMP as chain-transfer agent. Measurements were conducted at 60 °C using 1 wt% UVI 6976 as PAG. c) DSC measurement of DGEVA with 1 wt% imidazole as initiator (T**1**, red solid) and equimolar amounts (in respect to functional groups) of TMP and 1 wt% imidazole as catalyst (T**2**, purple dashed).

2. Results and Discussion

2.1. Coreactivity Study

Very recently, we have shown that the thermal reaction between epoxy and alcohol moieties as chain transfer agents (CTAs) is catalyzed by strong bases such as imidazoles and the reaction is proposed to proceed via a step-growth polyaddition.[27] In this recent study, a thorough kinetic investigation on the thermal polyaddition of epoxides with alcohols was conducted in bulk (using 1 wt% of imidazole as catalyst at 60 °C), highlighting the formation of polyadducts as the conversion of both functional groups proceeded in a similar pace. However, the reaction proceeded over a total of 6 h.

On the other side, the photochemical reaction between epoxy and alcohol monomers initiated by cationic species is well described in literature and follows the activated monomer (AM) mechanism, allowing hydroxyl species to be incorporated into an existing epoxy-derived poly(ether) network.[24,25] Although alcohols shift the reaction mechanism from activated chain end (ACE) to the activated monomer (AM) mechanism, polymerization is expected to proceed in a chain-growth fashion. For an even better understanding of the underlying photochemically initiated reaction, a combined photo-DSC and ^{1}H-NMR study of the reaction between monofunctional monomers (PGE and *n*-hexanol, equimolar ratio of functional groups) was conducted herein. The formulations furthermore contained 1 wt% of the sulfonium antimonate UVI6976 as cationic photoinitiator.

The main objective of this photo-DSC study was to elucidate the cationic co-polymerization behavior of epoxy:alcohol systems. Therefore, the respective formulations were irradiated in a controlled environment by means of the photo-DSC at 25 °C with filtered UV light (320–500 nm). The irradiation time was varied from 5 to 240 s and the respective conversion of each functional group was followed by the decrease of the corresponding peaks in the proton NMR spectra (Figures S1 and S2, Supporting Information).

The cationic photopolymerization of the epoxy-based phenyl glycidyl ether (PGE) and *n*-hexanol follows the chain-growth reaction type. The conversion of both monomers proceeds in a similar and linear fashion in the first 50 s of irradiation (**Figure** 4a) and full conversion (>98%) of both monomers was already reached after 1 min. Thereby, the fast and uniform formation of poly(ether)s via cationic ring-opening polymerization (CROP) was demonstrated. It has to be noted that one would expect a decrease in reaction rate over time. However, an almost linear trend of functional group conversion over time was observed in this study. The observed zero-order kinetic could be accounted to the fact that bulk-polymerizations are prone to volumetric shrinkage of the material. During polymerization, the monomeric bond distance is reduced from a van der Waals to a covalent bond distance, leading to volumetric shrinkage in the polymer and increasing

Table 1. Photo-DSC of DGEVA without (P**1**) and with (P**2**) the use of equimolar amounts (in respect to functional groups) of TMP as CTA using 1 wt% of UVI 6976 as PAG.

	Monomers	t_{max} [s]	t_{95} [s]	EGC_{IR} [%]
P1	DGEVA	8.6 ± 1.3	32.9 ± 2.3	63
P2	DGEVA + TMP	6.1 ± 0.4	32.5 ± 1.6	>99

the concentration of functional groups at any given time.[30] Furthermore, although the presence of hydroxyl groups enables the activated monomer (AM) mechanism, epoxy homopolymerization in the activated chain-end (ACE) fashion cannot be ruled out completely. Thereby, epoxy group conversion can be overestimated and can subsequently lead to a linear conversion over time.

Compared to the previously developed thermal epoxy-alcohol polyaddition,[27] a substantial decrease in reaction time was observed with the photochemical method herein. The thermal polymerization proceeded over a period of 6 h, however the photopolymerization showed full conversion of functional groups within 60 s.

2.2. Photochemical Cationic Ring-Opening Polymerization (CROP) Reactivity Study via (Photo-)DSC

After the assessment of the copolymerization of epoxy and alcohol monomers, a thorough comparison on polymerization kinetics of a multifunctional system was conducted. For this purpose, the light-induced cationic ring-opening polymerization (CROP) of the vanillin-based epoxy monomer DGEVA without (P**1**, "P" for photochemical) and with (P**2**) trimethylolpropane (TMP) as multifunctional chain-transfer agent (CTA) was investigated by means of photo-DSC. Again, the commercially available sulfonium antimonate-based PAG (UVI 6976) was used as initiator in 1 wt%. As the monomers DGEVA and TMP appear as white solids with melting points of around 55–58 °C, all investigations were performed at 60 °C. All samples were irradiated with a broadband UV lamp (320–500 nm, light intensity of 35 mW cm^{-2} at the sample surface) as the light source. Using the recorded heat of polymerization as a function of time, three key values were obtained from the analysis: t_{max} (time until the maximum heat development is reached), t_{95} (time to 95% of heat development) and the area of the peaks ΔH (total polymerization heat) were determined. Afterwards, the polymers were subjected to FT-IR analysis and the epoxy group conversions were determined according to Equation (1) (see Experimental Section).

The most important focus in this experiment was the impact of the CTA on the CROP of the epoxy monomer DGEVA. As can be seen in Figure 4b and **Table 1**, the addition of equimolar amounts of TMP (in respect to functional groups) reduced t_{max} from 8.6 s (P**1**) to 6.1 s (P**2**). This phenomenon also visible for t_{95} values: in the case of CROP (P**1**), t_{95} was higher (32.9 s) compared to P**2** (32.5 s). Hence, TMP acted as a powerful accelerator in the photoinduced cationic polymerization of DGEVA. Similar behavior can be found in literature, where TMP was used as a CTA for the CROP of BADGE and successfully increased photoreactivity.[31] Regarding the final epoxy group conversion (EGC), higher final EGC was determined via ATR-IR for P**2** (>99%) compared to the pristine DGEVA resin (P**1**, 63%). Kubisa and Penczek showed, that as a result of the AM mechanism, termination reactions seem to occur at a lesser extent compared to CROP without CTA.[23,24] Thus, the addition of a CTA increases the final epoxy group conversion. Additionally, considering that curing was conducted above the T_G of P**2** (48 °C, see 2.4.), but below the T_G of P**1** (84 °C, see 2.4.), the differences in EGC can be explained by their different chain mobilities at 60 °C. By increasing the curing temperature above the system's T_G, chain mobility is higher even in the late stages of the polymerization, resulting in higher EGC.[32] Thus, the topological limit was reached earlier for P**1**, additionally contributing to a decreased final conversion.

Table 2. DSC measurements of DGEVA with (T**2**) and without TMP (T**1**) as comonomer.

	Monomers	T_{onset} [°C]	T_{peak} [°C]	EGC_{IR} [%]
T1	DGEVA	98.2 ± 4.3	109 ± 2	61
T2	DGEVA+TMP	94.3 ± 0.6	111 ± 1	84

2.3. Thermal Anionic Ring-Opening Polymerization (AROP) Reactivity Study via DSC

The next step comprised a thermal reactivity study via DSC to investigate the potential for the imidazole-catalyzed anionic ring opening (AROP) of the neat epoxy monomer (T**1**, "T" for thermal) and step-growth polyaddition with trimethylolpropane (T**2**) were studied. The formulations consisted of 1 wt% of imidazole as catalyst combined with the monomers DGEVA (AROP) and DGEVA:TMP (polyaddition, equimolar ratio of functional groups). Measurements were performed with one heating cycle from 25 to -200 °C, gathering the following key values of the analysis: the onset temperature (T_{onset}) gives information about the lowest temperature at which a significant rise in heat of polymerization is detected, whereby the peak temperature T_{peak} defines the temperature with the maximum heat evolution. Additionally, upon integration of the exothermic peak, heat of polymerization is obtained. After the measurements, the EGC of the polymers was investigated via ATR-IR.

Herein, the addition of TMP (T**2**) to the neat epoxy monomer slightly decreased T_{onset} (94 °C) while T_{max} (111 °C) is similar to T**1** (T_{onset} 98 °C, T_{max} 109 °C), proposing that both polymerizations started at similar temperatures (Figure 4c, **Table 2**). Interestingly, the formulation T**2** showed a distinct endothermic peak at around 60 °C, caused by melting of solid components, while formulation T**1** remained liquid before the measurement started. When looking at the final EGC (determined via ATR-IR), polyaddition of DGEVA and TMP (T**2**) shows higher values (84%) compared to the AROP of the neat DGEVA (T**1**, 61%). Considering the step-wise character of the polyaddition, reactive chain ends are present up to high conversions, whereas in the AROP case, occurring termination reactions limit the final EGC.

2.4. Dynamic Mechanical Thermal Analysis (DMTA)

The final thermomechanical properties of polymer networks are affected by the underlying network architecture (Figure 4b,c) and

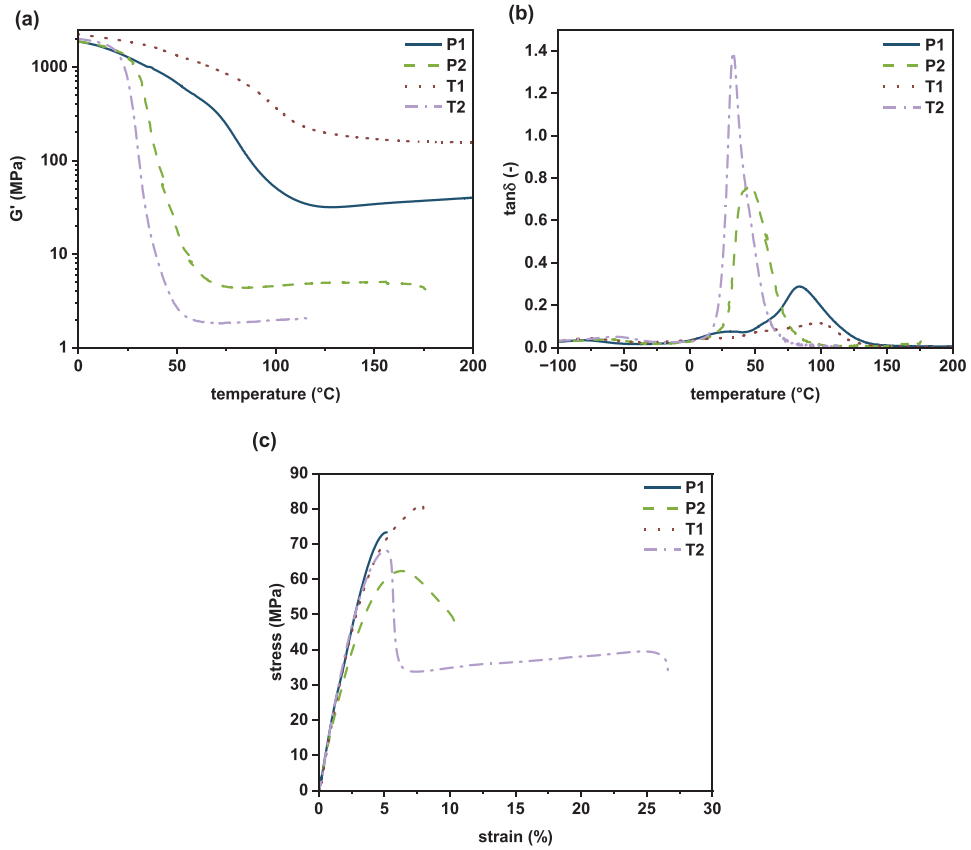

Figure 5. a) *G'* as a function of temperature and b) tanδ as a function of temperature of photochemically polymerized specimens P**1**–P**2** and thermally cured T**1**–T**2** networks. c) Tensile testing curves for photopolymerized DGEVA based polymers (P**1**–P**2**) and thermally cured networks T**1**–T**2**.

can be characterized using dynamic mechanical thermal analysis (DMTA). DMTA provides the impact of the monomer structure on the thermomechanical properties of polymer networks. The method is used to obtain the storage modulus (G'), loss modulus (G''), and the loss factor (tan δ) at different temperatures. The macroscopic glass transition (T_G) is associated with the loss factor and is dependent on various physicochemical and mechanical factors.[33] Moreover, the storage modulus at the rubbery plateau G'_r (measured at $T_G + 30$ °C) is an indication for the cross-linking density. G'_r was also used to extract the mesh size of the polymer networks L, that is inversely proportional to the crosslinking density of a material.[34,35] Results of all polymers are presented in **Figure** 5a,b and **Table** 3.

The specimens for thermomechanical tests were prepared via 2 preparation routes that differed mainly in the curing strategy. Photochemical CROP of DGEVA with and without the CTA was performed in a broadband UV oven (320–580 nm) at 60 °C, followed by a post-curing step at 90 °C for 18 h. This additional curing step was necessary to increase the final EGC of the specimens. Cations generated during irradiation are long-lived species, giving the cationic photopolymerization of epoxy monomers a living character.[36] By contrast, specimens containing imidazole as catalyst (1 wt%) were exclusively thermally cured for 18 h at 90 °C. Additionally, to test if the curing temperature influences the thermomechanical properties, specimens were prepared at 110 °C (UV curing and

Table 3. Overview of key parameters determined using DMTA and tensile testing of photochemically polymerized specimens P1–P2 and thermally cured T1–T2 networks.

	DMTA					Tensile testing		
	G'_{20} [MPa]	T_G [°C]	G'_r [MPa]	FWHM [°C]	L [nm]	σ_M [MPa]	ϵ_B [%]	U_T [MJ m^{-3}]
P1	1420	84	35.1	45	0.53	67.1 ± 5.8	5.19 ± 0.90	2.08 ± 0.17
P2	1470	48	4.38	27	1.03	63.2 ± 0.9	11.8 ± 3.2	5.45 ± 1.61
T1	1950	97	194	60	0.31	81.6 ± 7.3	8.71 ± 2.67	4.75 ± 1.84
T2	1400	35	1.85	19	1.36	66.9 ± 2.7	27.3 ± 2.8	10.0 ± 1.3

thermal (post)curing) and are displayed in Figure S3 (Supporting Information).

Prior to DMTA measurements, the conversion of the polymers was determined using FT-IR. For all specimens the oxirane ether band (≈915 cm^{-1}) in the IR spectra completely vanished after polymerization, indicating full conversion of the epoxy monomers for all types of polymerization.

Cationic photopolymerization of DGEVA (P1) exhibits a G'_{20} of 1.4 GPa reaching T_G at 84 °C with a FWHM (full width half maximum) of tanδ of 45 °C. G'_r of 35 MPa and L of 0.53 nm indicate that the matrix possesses high number of crosslinks. As previously discussed by Szczepanski et al. and Stanzione et al., the width of the tanδ is correlated with the homogeneity of polymer networks. Broad peaks indicate heterogeneous networks with a wide distribution of relaxation modes.[37,38] Hence, the broad FWHM of tanδ of P1 indicates inhomogeneous polymer networks, as a result of the unregulated (no CTA) CROP mechanism. When the initiating species is changed to a strong base (e.g., imidazole) and the epoxy monomers are polymerized in an anionic ring-opening fashion (T1), the highest G'_{20} of 1.9 GPa is obtained. T_G is also increased to 97 °C compared to the CROP material, although a broad FWHM of tanδ (60 °C) is determined. Taking FHWM of tanδ as parameter for network uniformity, inhomogeneity of the network is enhanced for AROP. In this regard, it is also not surprising that G'_r (194 MPa) exceeds and L (0.31 nm) is lower than P1, showing that AROP produces polymers with even higher crosslinking density. Crosslinking density is furthermore correlating to the amplitude of tanδ: lower amplitudes correlate to the tighter crosslinked networks.[33] Thus, presented data in Figure 5b emphasize the previously discussed trends, as the amplitude of T1 is distinctly lower than P1's peak height.

Adding a multifunctional alcohol (TMP) as CTA to the formulations clearly influences the thermomechanical properties of the (photo)polymerized material. In the case of P**2**, equimolar amounts of hydroxyl groups were added to the neat epoxy monomers DGEVA, altering the polymerization mode to the more regulated AM mechanism. A reduction in T_G (48 °C) is concomitant with a decrease in FWHM of tanδ (27 °C), while G'_{20} of 1.5 GPa is similar to P**1**. Previously, photo-DSC measurements already highlighted the superior final EGC and higher reactivity compared to polymers formed by the ACE mechanism (P**1**). Limiting conversion are often observed in photopolymerization of high T_G formulations.[25] As the network develops, a critical network density is reached above which a glassy polymer is obtained and propagation is slow, eventually hindering conversion increases.[39,40] Adding CTAs furthermore decreases the kinetic chain length of thermosets and consequently affects the crosslinking density.[41] Therefore, a significant reduction in G'_r (4.4 MPa) lead to higher L (1.03 nm) and overall lower concentration of crosslinks in the material. Hence, gathered data indicates a homogenization of the formed network architecture that however, comes along with reduction in T_G.

While CTAs enable network homogenization via reduction of the kinetic chain length,[25] base-catalyzed thermal epoxy-alcohol polyaddition (T**2**) uses an entirely different polymerization mechanism. As a result of a much slower step-growth reaction, the network build-up is regulated and the conversion at the gel point increased.[26] Thereby, the final (thermo)mechanical properties are affected. As previously presented by our group,[27] using a step-growth polyaddition leads to network homogenization of DGEVA when TMP is used as comonomer. Compared to the anionically homopolymerized T**1**, a decrease in T_G (35 °C) as well as G'_{20} (1.4 GPa) is observed, while FWHM of tanδ (19 °C) is significantly reduced to one third of T**1**'s value (60 °C), clearly outlining network homogenization. It has to be mentioned that T**2** was cured above its glass transition temperature (T_G 35 °C, curing at 90 °C). Thus, the polymer chains remained much more mobile during crosslinking and could thus additionally contribute to higher network homogeneity compared to T**1** (T_G 97 °C). Furthermore, the utilization of the step-growth mechanism alters the crosslinking density of a material. The chain-growth polymer T**1** shows both a lower tanδ amplitude and substantially higher G'_r values (194 MPa), than T**2** (1.9 MPa). Subsequently, a wider meshed material is obtained (L = 1.36 nm).

In summary, using alcohols as CTAs and polyaddition comonomers represent important tools to modify epoxy polymers. Comparable crosslinking densities ($L \approx 1$ nm) are achieved and network homogenization is evident in both cases with a narrowing of the tanδ_{max}.

2.5. Tensile Tests

To observe the impact of network homogenization and variation of the crosslinking density more closely, the stress-strain behavior of regulated compared to unregulated networks is particularly of interest. Therefore, tensile tests were conducted to extract key parameters such as maximum tensile strength (σ_M), elongation at break (ϵ_B) and tensile toughness (U_T). Measured results of the tensile testing are displayed in Figure 5c and Table 3. Furthermore, $\Delta\sigma/\Delta\epsilon$ values are displayed in Table S1 (Supporting Information).

The photopolymers containing 100 mol% DGEVA and no CTA (P**1**) show curve shapes typical for thermosets with a tensile strength of 67 MPa and low elongation at break of 5%. By integration of the stress-strain curves, a tensile toughness of 2 MJ m^{-3} is determined. On the other hand, using thermal AROP to obtain the polymer specimens (T**1**) gives a material of both higher σ_M (82 MPa) and ϵ_B (9%), resulting in a twofold increase in ultimate tensile toughness (4.75 MJ m^{-3}). Although both P**1** and T**1** show brittle fracture behavior, the higher T_G and crosslinking density in the latter case seem to boost the final mechanical properties of the material.

A totally different stress–strain behavior is observed for the photopolymerized P**2** containing TMP as CTA. While the tensile strength drops slightly to 63 MPa, a distinct yield point and two-times higher elongation at break (12%) compared to P**1** is displayed in Figure 5c. Thereby, the tensile toughness of the polymer is nearly three-times higher (5.5 MJ m^{-3}) than for the polymers containing no CTAs. Clearly, network homogenization and lower crosslinking density of the materials effect the mechanical properties of the material. Notably, tensile tests were performed at 25 °C. At this temperature, tanδ of P**2** starts to rise (Figure 5b) and thereby, the polymer starts to emerge into a more rubbery-like material during glass-transition.

This transition towards the rubbery state is even more pronounced for the thermally cured T**2** (T_G of 35 °C). Polyaddition of DGEVA and TMP leads to even higher ϵ_B (27%), while σ_M

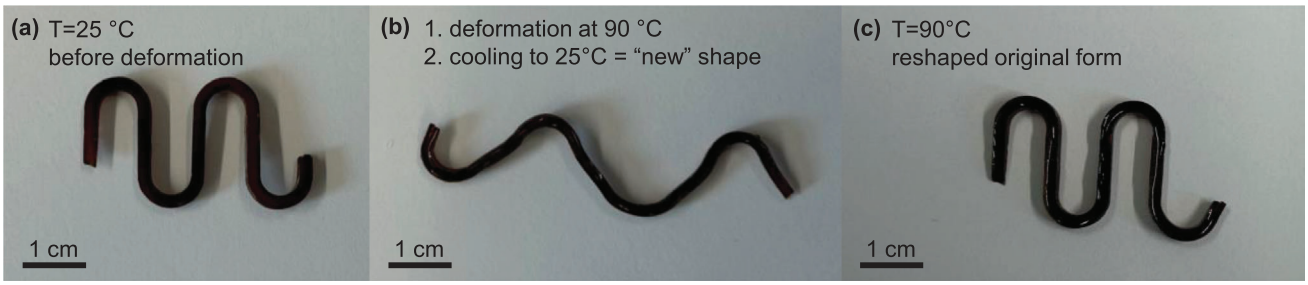

Figure 6. Scheme of the shape-memory behavior of polymer samples. a) A polymer specimen of T2 formed into a serpentine line at $T < T_G$. b) The specimen is heated above its TG to 90 °C, stretched and thereafter cooled to 25 °C. c) T2 after re-heating to 90 °C: the original shape was regained.

(67 MPa) remains unaffected compared to the CTA-polymer P**2**. Unsurprisingly, highest tensile toughness (10 MJ m^{-3}) is determined for T**2**.

All in all, it can be concluded that the addition of hydroxyl species to epoxy monomers leads to a reduction in crosslinks that result in network homogenization and enhanced tensile toughness. Noteworthy, using a step-growth polymerization even exceeds the effects of CTAs, making epoxy-alcohol polyaddition a novel tool for both network regulation and toughness enhancement.

2.6. Shape-Memory Properties of Epoxy-Alcohol Polyadducts

Thermo-responsive shape-memory polymers have attracted huge interest because of their unique ability of remembering their shape. Recently, the vanillin-core structure that is present in DGEVA has attracted considerable attention to produce materials with shape memory behavior.[42,43] While P**1**–P**2** and T**1** did not show the ability of shape memory, the thermal polyadduct T**2** turned out to be an excellent candidate. In order to show shape-memory properties, one polymer specimen of T**2** in a serpentine line form (**Figure 6a**) was heated above its T_G (35 °C) to 90 °C, reformed to a temporary stretched shape and immediately cooled to room temperature (Figure 6b). The specimen was able to maintain its temporary shape at this temperature, but heating to 90 °C led to a spontaneous (<10 s) return to the original wavy shape (Figure 6c). For better visualization of the shape memory properties of T**2**, Video S1 (Supporting Information) shows the effect in real time.

3. Conclusion

In this study, the lignin-derived epoxy monomer DGEVA was polymerized in four different ways: cationic photopolymerization with and without CTAs, thermal anionic polymerization and base-catalyzed thermal polyaddition. The (photo)reactivity as well as thermomechanical properties of all polymers were assessed. Firstly, the cationic photopolymerization was analyzed using photo-DSC. In a coupled study with proton NMR measurements, it was shown that multifunctional alcohols act as CTAs and both monomers convert homogeneously over time with a rate of polymerization of 16.5 mol L^{-1} s^{-1}. Additionally, the addition of CTAs led to increased photoreactivity (t_{max} of 6 s, t_{95} of 32 s), while simultaneously enhancing the final conversion of the epoxy monomers (>80%). In a DSC study, the anionic homopolymerization via AROP was compared to the thermally initiated epoxy-alcohol polyaddition. Again, the addition of equimolar amounts of hydroxyl groups to a neat epoxy resin enhanced the final conversion (>80%) with onset temperatures of 90 °C and peak temperatures of 110 °C. Most important information was gathered during DMTA, as the addition of alcohols did not only lead to significant network homogenization (FWHM of $\tan\delta_{max}$ of 20–27 °C) but also to reduced crosslinking densities (G'_r of 1.8–4.4 MPa). The change network architecture has a direct impact on stress–strain behavior of the material. Traditional CROP and AROP gave brittle polymers (σ_M up to 80 MPa, ϵ_B <10%), but adding alcohols either as CTAs or comonomers into the networks resulted in a substantial increase in elongation at break (up to 27%) and concomitantly also in increased tensile toughness (up to 10 MJ m^{-3}). Finally, polymers derived from epoxy-alcohol polyaddition turned out to be promising candidates as shape-memory materials.

4. Experimental Section

Materials and General Methods: Vanillyl alcohol (TCI Europe), epichlorohydrin (Sigma-Aldrich), tetrabutylammonium chloride (TCI Europe), sodium hydroxide (Sigma-Aldrich), phenyl glycidyl ether (Sigma-Aldrich), n-hexanol (Sigma-Aldrich), 1,6-hexanediol (Sigma-Aldrich), trimethylolpropane (ACROS), imidazole (Fluka), and pyridine (TCI Europe) were purchased from the respective companies and used without further purification. The photoinitiator Cyracure UVI6976 was purchased from Univar Products International.

Column chromatography was performed on a Büchi Sepacore Flash System (Büchi pump module C-605, Büchi control unit C-620, Büchi UV-Photometer C-635, Büchi fraction collector C-660), using glass columns packed with silica gel (Merck). Ethyl acetate and petroleum ether were used as eluents and received from Donau Chemie.

NMR-spectra were recorded on a Bruker Avance DRX-400 FT-NMR spectrometer at 400 MHz for ^{1}H- and 100 MHz for ^{13}C-NMR spectra. The signals are reported with their chemical shifts in ppm and fine structure (s = singlet, d = doublet, t = triplet, q = quartet, qn = quintet, sep = septet, m = multiplet). The chemical shifts were indicated in ppm relative to trimethyl silane ($d = 0$ ppm) and referenced by using the respective NMR solvent [^{1}H: $CDCl_3$ (7.26 ppm), DMSO-d_6 (2.54 ppm) ^{13}C: $CDCl_3$ (77.16 ppm)] as internal reference.

Melting points were measured on an OptiMelt automated melting point system from SRS Stanford Research System. The heating rate was set to 1 °C min^{-1}.

Synthesis of Diglycidyl Ether of Vanillyl Alcohol (DGEVA): For this study, a diglycidyl derivative of vanillyl alcohol was prepared in analogy to Fache

et al.[16] A detailed synthetic procedure can be found in the Supporting Information.

Formulation and Specimen Preparation: For the proton NMR study, (photo-)DSC, DMTA and tensile test measurements formulations were prepared using 1 wt% of the respective initiator (imidazole for thermal curing and Cyracure UVI6976 for photopolymerization). If necessary, the formulations were heated to 60 °C to melt solid components and homogenized using a vortex mixer. For the (photo-)DSC measurements and proton NMR study, all formulations were directly used after preparation. For (thermo)mechanical measurements, the thermally curable monomer formulations were casted in silicone molds (sticks, $5 \times 2 \times 40$ mm^3 for DMTA; dog-bone-shaped samples in accordance with ISO 527 test specimen 5b, total length of 35 mm and a parallel region of $2 \times 2 \times 2$ mm^3 for tensile tests) at 90 °C for 18 h. Photoreactive formulations were polymerized at 60 °C in an Uvitron UV 1080 Flood Curing oven equipped with Uvitron Intelliray 600 halide lamps at 50% intensity (approximately 60 mW cm^{-2}) with an unfiltered spectral range from 320 to 580 nm for 5 min. Thereafter, the specimens were post-cured at 90 °C for 18 h. The polymer specimens were ground to obtain uniform specimens with exact dimensions (deviations $\leq \pm 0.1$ mm).

FT-IR Spectroscopy: Conversion of the epoxy moieties was determined by FT-IR spectroscopy by analysis of the change of the integral of the epoxy ring vibration (≈910 cm^{-1}) in reference to the integral of the aromatic ring vibration (≈800 cm^{-1}).[44]

$$\text{Epoxy group conversion} \quad (\%) = \left(1 - \frac{\frac{A_{\text{epoxy,polymer}}}{A_{\text{ref,polymer}}}}{\frac{A_{\text{epoxy,monomer}}}{A_{\text{ref,monomer}}}}\right) \cdot 100\% \tag{1}$$

where $A_{\text{epoxy,polymer/monomer}}$ is the area of the epoxy signal at ≈910 cm^{-1} in the polymer/monomer and $A_{\text{ref,polymer/monomer}}$ is the area of the reference band at ≈800 cm^{-1} in the polymer/monomer.

Proton NMR Study: Formulations of around 1 g were composed as follows: monofunctional epoxy (PGE) and alcohol (*n*-hexanol) monomers were mixed in a 50 mol% ratio (in respect to functional groups) and 1 wt% of the cationic photoinitiator Cyracure UVI6976 was added. Irradiation of the samples was conducted using a Netzsch DSC 204 F1 Phoenix equipped with an autosampler and a double-core glass-fiber light guide (diameter = 3 mm). 10–12 mg of the formulation were weighed in standard aluminum crucibles and closed with glass lids to prevent evaporation. All measurements were performed under a N_2 flow of 20 mL min^{-1} at 60 °C. After an isothermal phase of 5 min, the crucibles were irradiated for 5, 10, 15, 20, 25, 30, 35, 40, 45, 50, 60, 90, 120 and 240 s with an Exfo OmniCure 2000 device with a spectral range of 320–500 nm. The light intensity on the surface was set to 35 mW cm^{-2}. The measurements were conducted at 25 °C. After the measurement, the samples were immediately quenched with 1 drop of pyridine to prevent dark-curing and dissolved in ≈0.7 mL of the NMR solvent.

The conversion of both epoxy and alcohol moieties was followed by the decrease of the respective signal integral over time, using Equation (2). The corresponding NMR spectra are depicted in Figure S2 (Supporting Information).

$$\text{Conversion} \quad (\%) = \left(1 - \frac{\text{integral}\ (t_x)}{\text{integral}\ (t_0)}\right) \cdot 100\% \tag{2}$$

where integral (t_x) is the area of the corresponding peaks at time points $t = t_x$ and integral (t_0)is the area of the corresponding peaks prior to the reaction

The rate of polymerization (R_p) was determined according to Equation (3). Therefore, monomer conversion (%) was plotted against the reaction time (s) and the slope of the graph gave the rate of polymerization ($R_{p,s}$) in s^{-1}, which describes the conversion of the monomer per time (s). To obtain the rate of polymerization as the concentration (mol L^{-1}) per time (s), the density (ρ in g L^{-1}) and molecular mass (g mol^{-1}) of the monomer were used. The density of the monomers was determined by using a pycnometer with an exact volume of 1 mL.

$$R_p \left[\frac{\text{mol}}{L \cdot s}\right] = \frac{R_{p,s}\,[1/s] \cdot \rho \left[\frac{g}{L}\right]}{M \left[\frac{g}{\text{mol}}\right]} \tag{3}$$

where R_p is the rate of polymerization [mol L^{-1} s^{-1}], $R_{p,s}$ is the rate of polymerization derived from the slope of conversion per time graph [s^{-1}], ρ is the density of the monomer at 60 °C [g L^{-1}], and M is the molecular weight of the monomer [g mol^{-1}].

Reactivity Study via (Photo-)DSC: For the assessment of the thermal curing behavior, about 10 mg (with an accuracy of ±0.1 mg) of each formulation were weighed in an aluminum pan and subsequently sealed with an aluminum lid. An empty pan was used as reference. The measurements were conducted on a simultaneous thermal analyzer (STA 449 F1 Jupiter, NETZSCH), and the temperature was raised from 25 to 200 °C with a heating rate of 5 K min^{-1}. For analysis of the DSC plots, the onset of the exothermal peak was evaluated by laying tangents and intersecting them. Heat of reaction was determined through the integration of heat flow over the exothermal peak. All measurements were conducted in duplicates, and the results were averaged. For the photoreactivity, photo-DSC measurements were conducted as mentioned above. Samples were irradiated for 300 s at 60 °C and measurements were conducted in triplicates to ensure reproducibility.

Dynamic Mechanical Thermal Analysis (DMTA): Dynamic mechanical thermal analysis (DMTA) measurements were performed with an Anton Paar MCR 301 with a CTD 450 oven and an SRF12 measuring system. The polymer specimens were tested in torsion mode with a frequency of 1 Hz and a strain of 0.1%. The temperature was increased from −100 to 200 °C with a heating rate of 2 °C min^{-1}. The storage modulus (G') and loss factor (tan δ) curves were processed with the software Rheoplus/32 V3.40 from Anton Paar. The glass transition temperature (T_G) was obtained from the maximum of the loss factor (tan δ_{max}). Additionally, G' at the rubbery plateau (G'_r) and full width at half maximum (FWHM) of tan δ_{max} were determined.

$G'r$ was used to calculate the average mesh size L of the networks as a measure for the crosslinking density of polymer networks by Equation (4).[35]

$$L = \left(\frac{R \cdot T}{G'_r \cdot N_A}\right)^{1/3} \tag{4}$$

where L is the average mesh size [nm], R is the molar gas constant [J K^{-1} mol^{-1}], T is the temperature at which G'_r was determined (T_G + 30 °C) [K], G'_r is the storage modulus at the rubbery plateau [Pa] and N_A is the Avogadro number [mol^{-1}].

Tensile Tests: Tensile tests were performed on a Zwick Z050 tensile machine, which reaches a maximum test force of 50 kN. The samples were strained with a crosshead speed of 5 mm min^{-1} and a maximum force of 1 kN. During the measurement, a stress–strain plot was recorded for analysis. Six specimens were tested per formulation with satisfactory reproducibility.

Shape Memory: For the shape-memory experiments, a formulation consisting of equimolar amounts (regarding functional groups) of DGEVA and TMP was cured at 90 °C for 18 h using 1 wt% of imidazole as catalyst. To demonstrate the shape memory behavior, the polymer sample was heated to 90 °C with a water bath, stretched and immediately cooled to 25 °C (using a water bath). Following, the deformed specimen was subjected into a hot water bath (90 °C).

Supporting Information

Supporting Information is available from the Wiley Online Library or from the author.

Acknowledgements

Funding by the Christian Doppler Research Association within the framework of the "Christian Doppler Laboratory for Advanced Polymers for Biomaterials and 3D Printing" and the financial support by the Austrian Federal Ministry for Digital and Economic Affairs and the National foundation for Research, Technology and Development are gratefully acknowledged. The authors acknowledge TU Wien Bibliothek for financial support through its Open Access Funding Programme.

Conflict of Interest

The authors declare no conflict of interest.

Data Availability Statement

The data that support the findings of this study are available from the corresponding author upon reasonable request.

Keywords

biobased epoxy resin, photopolymerization, polyaddition, sustainable epoxy resin

Received: May 8, 2024
Revised: August 12, 2024
Published online:

[1] A. Gandini, *Green Chem.* **2011**, *13*, 1061.
[2] V. S. D. Voet, J. Guit, K. Loos, *Macromol. Rapid Commun.* **2021**, *42*, 2000475.
[3] R. Auvergne, S. Caillol, G. David, B. Boutevin, J.-P. Pascault, *Chem. Rev.* **2014**, *114*, 1082.
[4] F. Ng, G. Couture, C. Philippe, B. Boutevin, S. Caillol, *Molecules* **2017**, *22*, 149.
[5] J. Wan, J. Zhao, X. Zhang, H. Fan, J. Zhang, D. Hu, P. Jin, D.-Y. Wang, *Prog. Polym. Sci.* **2020**, *108*, 101287.
[6] B. M. Bell, J. R. Briggs, R. M. Campbell, S. M. Chambers, P. D. Gaarenstroom, J. G. Hippler, B. D. Hook, K. Kearns, J. M. Kenney, W. J. Kruper, D. J. Schreck, C. N. Theriault, C. P. Wolfe, *CLEAN – Soil, Air, Water* **2008**, *36*, 657.
[7] L. N. Vandenberg, R. Hauser, M. Marcus, N. Olea, W. V. Welshons, *Reprod. Toxicol.* **2007**, *24*, 139.
[8] X. Pan, P. Sengupta, D. C. Webster, *Biomacromolecules* **2011**, *12*, 2416.
[9] M. Stemmelen, F. Pessel, V. Lapinte, S. Caillol, J. P. Habas, J. J. Robin, *J. Polym. Sci., Part A: Polym. Chem.* **2011**, *49*, 2434.
[10] D. S. Branciforti, S. Lazzaroni, C. Milanese, M. Castiglioni, F. Auricchio, D. Pasini, D. Dondi, *Addit. Manuf.* **2019**, *25*, 317.
[11] C. Mantzaridis, A.-L. Brocas, A. Llevot, G. Cendejas, R. Auvergne, S. Caillol, S. Carlotti, H. Cramail, *Green Chem.* **2013**, *15*, 3091.
[12] M. Chrysanthos, J. Galy, J.-P. Pascault, *Polymer* **2011**, *52*, 3611.
[13] J. Cheng, P. Zhang, T. Liu, J. Zhang, *Polymer* **2015**, *78*, 212.
[14] X. Feng, A. J. East, W. B. Hammond, Y. Zhang, M. Jaffe, *Polym. Adv. Technol.* **2011**, *22*, 139.
[15] S. Laurichesse, L. Avérous, *Prog. Polym. Sci.* **2014**, *39*, 1266.
[16] M. Fache, R. Auvergne, B. Boutevin, S. Caillol, *Eur. Polym. J.* **2015**, *67*, 527.
[17] M. Fache, B. Boutevin, S. Caillol, *ACS Sustainable Chem. Eng.* **2016**, *4*, 35.
[18] Z. Wang, P. Gnanasekar, S. Sudhakaran Nair, R. Farnood, S. Yi, N. Yan, *ACS Sustainable Chem. Eng.* **2020**, *8*, 11215.
[19] E. Savonnet, E. Grau, S. Grelier, B. Defoort, H. Cramail, *ACS Sustainable Chem. Eng.* **2018**, *6*, 11008.
[20] R. Dinu, U. Lafont, O. Damiano, A. Mija, *ACS Appl. Polym. Mater.* **2022**, *4*, 3636.
[21] C. Noè, S. Malburet, A. Bouvet-Marchand, A. Graillot, C. Loubat, M. Sangermano, *Prog. Org. Coat.* **2019**, *133*, 131.
[22] S. C. Ligon-Auer, M. Schwentenwein, C. Gorsche, J. Stampfl, R. Liska, *Polym. Chem.* **2016**, *7*, 257.
[23] P. Kubisa, M. Bednarek, T. Biedroń, T. Biela, S. Penczek, *Macromol. Symp.* **2000**, *153*, 217.
[24] P. Kubisa, S. Penczek, *Prog. Polym. Sci.* **1999**, *24*, 1409.
[25] B. Dillman, J. L. P. Jessop, *J. Polym. Sci., Part A: Polym. Chem.* **2013**, *51*, 2058.
[26] J. D. McCoy, W. B. Ancipink, S. R. Maestas, L. R. Draelos, D. B. Devries, J. M. Kropka, *Thermochim. Acta* **2019**, *671*, 149.
[27] A. Fantoni, T. Koch, S. Baudis, R. Liska, *ACS Appl. Polym. Mater.* **2023**, *5*, 731.
[28] A. Fantoni, J. Ecker, M. Ahmadi, T. Koch, J. Stampfl, R. Liska, S. Baudis, *ACS Sustainable Chem. Eng.* **2023**, *11*, 12004.
[29] D. Foix, X. Ramis, F. Ferrando, A. Serra, *Polym. Int.* **2012**, *61*, 727.
[30] T. Takata, T. Endo, in *Expanding Monomers: Synthesis, Characterization, and Applications*, (Eds: R. M. Luck, R. K. Sadhir), Vol. *1*, CRC Press, Boca Raton, FL **1992**, p. 416.
[31] C. Dall'Argine, A. Hochwallner, N. Klikovits, R. Liska, J. Stampf, M. Sangermano, *Macromol. Mater. Eng.* **2020**, *305*, 2000325.
[32] W. D. Cook, *Polymer* **1992**, *33*, 2152.
[33] I. M. Kalogeras, H. Hagg Lobland, *J. Mater. Educ.* **2012**, *34*, 69.
[34] C. Gorsche, K. Seidler, P. Knaack, P. Dorfinger, T. Koch, J. Stampfl, N. Moszner, R. Liska, *Polym. Chem.* **2016**, *7*, 2009.
[35] J. Wang, V. M. Ugaz, *Electrophoresis* **2006**, *27*, 3349.
[36] V. Sipani, A. B. Scranton, *J. Polym. Sci., Part A: Polym. Chem.* **2003**, *41*, 2064.
[37] C. R. Szczepanski, C. S. Pfeifer, J. W. Stansbury, *Polymer* **2012**, *53*, 4694.
[38] J. F. Stanzione, K. E. Strawhecker, R. P. Wool, *J. Non-Cryst. Solids* **2011**, *357*, 311.
[39] T. Scherzer, U. Decker, *Polymer* **2000**, *41*, 7681.
[40] C. Decker, K. Moussa, *J. Appl. Polym. Sci.* **1987**, *34*, 1603.
[41] G. Odian, *Principles of Polymerization*, Wiley, New York **2004**.
[42] Y. Tian, Q. Wang, Y. Hu, H. Sun, Z. Cui, L. Kou, J. Cheng, J. Zhang, *Polymer* **2019**, *178*, 121592.
[43] J. Jaras, A. Navaruckiene, E. Skliutas, J. Jersovaite, M. Malinauskas, J. Ostrauskaite, *Polymers* **2022**, *14*, 2460.
[44] T. Theophile, *Infrared Spectroscopy: Materials Science, Engineering and Technology*, IntechOpen, London **2012**.

